Microchemical Journal 142 (2018) 394–402

Contents lists available at ScienceDirect

Microchemical Journal

journal homepage: www.elsevier.com/locate/microc

Bioactive assay and hyphenated chromatography detection for complex supercritical CO_2 extract from *Chaihu Shugan San* using an experimental design approach

Min He[a,*], Liang Hong[a], Zhi-Yu Yang[a,b], Tian-Biao Yang[a], Jun Zeng[a]

[a] Department of Pharmaceutical Engineering, School of Chemical Engineering, Xiangtan University, Xiangtan 411105, People's Republic of China
[b] Medical Metabolic International Collaborative Center, Xiangya Hospital, Central South University, Changsha 410008, People's Republic of China

ARTICLE INFO

Keywords:
Chaihu Shugan san
Supercritical carbon dioxide extraction
ACGWO
LC-MS-IT-ToF
Anti-inflammatory
Antioxidant

ABSTRACT

In this study, Super Critical CO_2 (SCC) was applied to extract the active ingredients from Multi-herbal formula *Chaihu Shugan San* (CSS). Response Surface Methodology (RSM) coupled with an improved chaotic Gray Wolf Optimization (ACGWO) was employed to the experimental design. After gas chromatography–mass spectrometer (GC–CI/EI-MS) detection, liquid chromatography–mass spectrometry- ion trap-time of flight (LC–MS-IT-ToF) further indicated that several phthalides are mainly responsible for the SCC extract; the next is α-Cyperone in *Cyperus rotundus*; and Meranzin hydrate, Isomeranzin in *Citrus reticulata Blanco* again. Further pharmacological tests were also performed for the SCC extracts. THP-1 macrophages were used to observe the anti-inflammatory effects. The expression of IL-6 was obviously suppressed by the SCC extract from CSS, through a positive correlation with the dose. Then, ROS content in a cell model was used to detect the antioxidant capacities. The results showed that the SCC extract from CSS, exert dose-dependent inhibitory effects on the oxidative stress of the cells.

1. Introduction

The different combination of herbs can be found in traditional Chinese medicine (TCM) or functional food. *Chaihu Shugan San* (CSS), one of the typical representatives, is mainly used for the diseases like mental disorders, liver diseases [1, 2]. CSS formula is consisting of *Pericarpium citri reticulatae*, *Radix bupleuri*, *Ligusticum chuanxiong hort*, *Rhizoma cyperi*, *Fructus aurantii*, *Paeonia lactiflora* and *Glycyrrhiza uralensis fisch*, in which the semi-volatile Phthalides and Terpenoids are two of the most important ingredients [3]. Nevertheless, the traditional decocting method was mainly accounts for the extracts of seven herbs, which easily cause the degradation and isomerization of those compounds.

At present, many methods are applied to separate the bio-active constituents from herbs, including hydro-distillation [4], microwave-assisted extraction [5], continuous subcritical water extraction [6], ultrasonic extraction [7], etc. These methods are time-consuming and environmental unfriendly. In contrast, supercritical CO_2 (SCC) extraction has been widely used in the separation of effective substances in natural products [8], due to its environment friendly, low temperature operation, and so on. The Extraction Yield (EY) is usually influenced by multiple factors in SCC extraction. The experimental design [9] is aims to explain the factors under conditions that are hypothesized to reflect the variation. There are many chemometric methods utilized to analyze the interaction between these factors and results, including Response Surface Methodology (RSM) [10], Excel [11], Taguchi Design Method [12]. Among them, RSM based on Small Face Central Composite Design (SFCCD) has been widely used to optimize various operating parameters of the extraction process, as well as the EY modeling. The ideal RSM results indicated that the experimental data can be applied to a mathematical equation, which is an effective statistical model [13]. In the past years, some good statistical approaches were used, such as Gray Wolf Optimization (GWO) [14], Particle Swarm Optimization (PSO) [15], genetic algorithm [16], and hybrid particle swarm-ant colony algorithm [17], etc. Here, GWO algorithm enjoys simple principle, few adaptable parameters, fast convergence speed and good global search capability, which can be applied in the supercritical process [18]. However, GWO also has many disadvantages, such as, an over-reliance on the initial population, premature convergence, prone to local optimum and the unstable convergence process.

Since CSS extract is multi-components mixtures, the chemical identification is thus of great importance, not only for the clarification

* Corresponding author.
E-mail addresses: hemin1976@xtu.edu.cn, dahai8214813@gmail.com (M. He).

https://doi.org/10.1016/j.microc.2018.07.016
Received 7 June 2018; Received in revised form 14 July 2018; Accepted 15 July 2018
Available online 18 July 2018
0026-265X/

of pharmacodynamic basis, but also for providing scientific evidence for the quality control. Because of efficient separation and abundant information, Mass Spectrometry (MS) coupled with Liquid Chromatography (LC) or Gas Chromatography (GC) has been used to identify the composition in herb or food [19]. Due to the herbal complexity, the chemometric resolution and some *in-silico* approaches have been introduced in the data analysis of GC–MS and LC–MS [20]. These methods provide an accurate, fast, cheap quantitative analysis in the presence of heavy interference by other analytes.

Further pharmacological tests should also be performed for the TCM formula or their extracts. Kuai et al. found that Sheng-ji Hua-yu formula can promote the diabetic wound healing of re-epithelization [21]. Sui et al provided the first direct evidence demonstrating Zhi-Zhen-Fang can attenuate multidrug resistance by repressing Hedgehog signaling [22]. The study by Zhou et al. indicated that Huolingshengji Formula possess neuroprotective effects in SOD1G93A mouse model [23]. Many herbs have been proved to possess anti-inflammatory [24, 25] and antioxidant activity [26, 27]. However, the TCM Formula is too complex, their pharmacological activities can't be explained clearly. Therefore, the multi-angle, multi-level study of different extracts should be adopted in the bioactivity researches of TCM Formula.

The paper discussed the experimental procedure of the SCC extraction from the formula CSS. In this procedure, the EY model was optimized by an improved chaotic Gray Wolf Optimization (ACGWO) algorithm. After the morphological examination of herbal particles, the chemical composition was analyzed by GC–MS and LC–MS apparatus. Finally, the anti-inflammatory and antioxidant researches were performed in the SCC extracts from CSS formula.

2. Material and methods

2.1. Materials

The herbs, such as *Pericarpium citri reticulatae*, *Radix bupleuri*, *Ligusticum chuanxiong hort*, *Rhizoma cyperi*, *Fructus aurantii* and *Paeonia lactiflora*, were purchased from Hunan Academy of Chinese Medicine. The crude herbs were air-dried indoors before smashing into several grades. CO_2 (99.9%) was provided by Chang Gang gas Co. Ltd. (Changsha, China). Alkane standard solutions of C_8-C_{20} (no. 04070) were purchased from Fluka Chemika (Buchs, Switzerland). Ligustilide and α-Cyperone were purchased from the Chinese National Institute for Control of Pharmaceutical and Biological Products (Beijing, China). A human monocytic leukemia cell line (THP-1) and HepG2 cells were purchased from American Type Culture Collection (ATCC, USA). Lipopolysaccharide (LPS), RPMI 1640 medium were purchased from Sigma-Aldrich and Thermo Fisher companies, respectively. Human IL-6 ELISA kit and human TNF- α kit were purchased from Enzo life sciences, Inc. H_2O_2 was purchased from Kun Feng Chemical Co., Ltd. (Jinan, China). DCFH-DA fluorescent probe (Invitrogen A/S Taastrup, Denmark). DMSO and Celecoxib was purchased from Macklin Biochemical company (Shanghai, China) and Pfizer pharmaceuticals Ltd. (New York, America). Penicillin and streptomycin were purchased in XiangTan central hospital. The solvents, such as methanol and n-Hexane, were of HPLC grade.

2.2. Supercritical CO_2 extraction

A supercritical CO_2 extraction device (Fig. S I1, Supplemental information I), HA121-50-01, was supplied by HuaAn Supercritical fluid extraction Co. Ltd. (Nantong, China). The extraction system is consisted of one 1 L extraction vessel and two separators. The gas tank with a condenser can offer CO_2 fluid, and the output can be increased to the desired pressure by a pump. In this study, 150 g of dried herbs was loaded into a 1 L high pressure vessel, and the liquid CO_2 was used to extract the essential oil. Later, the extracts were fed into the separator I and separator II, in which the density of CO_2 and the solubility of essential oil could be adjusted by various pressure. Every 60 min in separator II, the liquid oil was released completely from the gaseous CO_2, and the latter was flowed into a purifier for recycled use. Finally, the weighed essential oil was stored in −20 °C for further analysis. The extraction yield (EY) can be calculated in accordance with Eq. (1).

$$EY(\%) = \frac{W_{oil}}{W_{powder\ of\ CSS}} \times 100\% \quad (1)$$

W_{oil} refers to the weight of oil, $W_{powder\ of\ CSS}$ refers to the weight of herbs.

2.3. Experimental design, RSM prediction and ACGWO optimization

Many parameters may influence the EY of CSS either directly or indirectly. However, traditional single factor design requires many experiments, and often ignore the interaction between the various factors. In our study, three factors (extraction temperature, extraction pressure and particle size) are utilized to investigate their influences on EY. The remaining parameters are specified at the fixed values, such as extraction time at 120 min, CO_2 flow rate at 43.67 L/h, and weight of CSS powder was specified as 150 g.

In our study, RSM was applied to analyze the relationships between three input independent variables and the output parameter. After three-factor three-level values in this experiment are set, the experiment is designed by the Small Face Central Composite Design (SFCCD) based on the 15 sets of operating parameters, including four factorial points, six axial points and five center points. When it comes to the experimental results, analysis of variance (AOV) was used to calculate the statistical significance of each coefficient on EY. A nonlinear fitting method was then used to establish the quadratic polynomial regression equation, which was introduced to predict the highest yield.

GWO algorithm is applied to achieve the simulation by building a 4-layer pyramid hierarchical management system, which performs the social hunting behavior. The management system is divided into α (the first layer), β (the second layer), δ (the third layer), ω (the fourth layer). The GWO principle (Supplemental information II) is a novel meta-heuristic algorithm for global optimization, and the position of the prey is the optimal solution after multiple iterations. To maintain the diversity of the population and make the initial population uniformly distributed, the chaotic algorithm was introduced in GWO algorithm (Fig. S II1, Supplemental information II) to accelerate the convergence speed of the algorithm. Chaos randomness and ergodicity can avoid the tendencies of falling into local minimal values during the search process, thus overcoming the shortcomings of GWO algorithm. Furthermore, the coordinated problem between global search and local search were common in the group intelligence algorithms. The strong global search ability can ensure the diversity of the population, and the strong local search capability can guarantee the precision of results. Therefore, it is important to deal with the balance between the global search capability and the local search capability in the GWO algorithm. The linear convergence of the convergence factor *a* can't fully reflect the actual optimization process. To maintain the balance between global search and local search, a nonlinear convergence factor was introduced in the algorithm (Fig. S II2, Supplemental information II).

As observed in Fig. 1, the optimization steps of ACGWO algorithm are explained. Firstly, the algorithm parameters were set. Secondly, the fitness values of individuals in the population are calculated, then the first three values with better fitness are assigned to α, β and δ. Thirdly, the position of ω and the chaotic sequence are updated. Fourthly, the number of iterations and convergence factor *a* were updated, to calculate the value of the improved $\vec{a}$ and update the parameters ($\vec{r_1}$, $\vec{r_2}$, $\vec{a}$, $\overrightarrow{C_{id}}$, $\overrightarrow{A_{id}}$ and X_n) etc. Finally, the optimal solution (α) could be obtained.

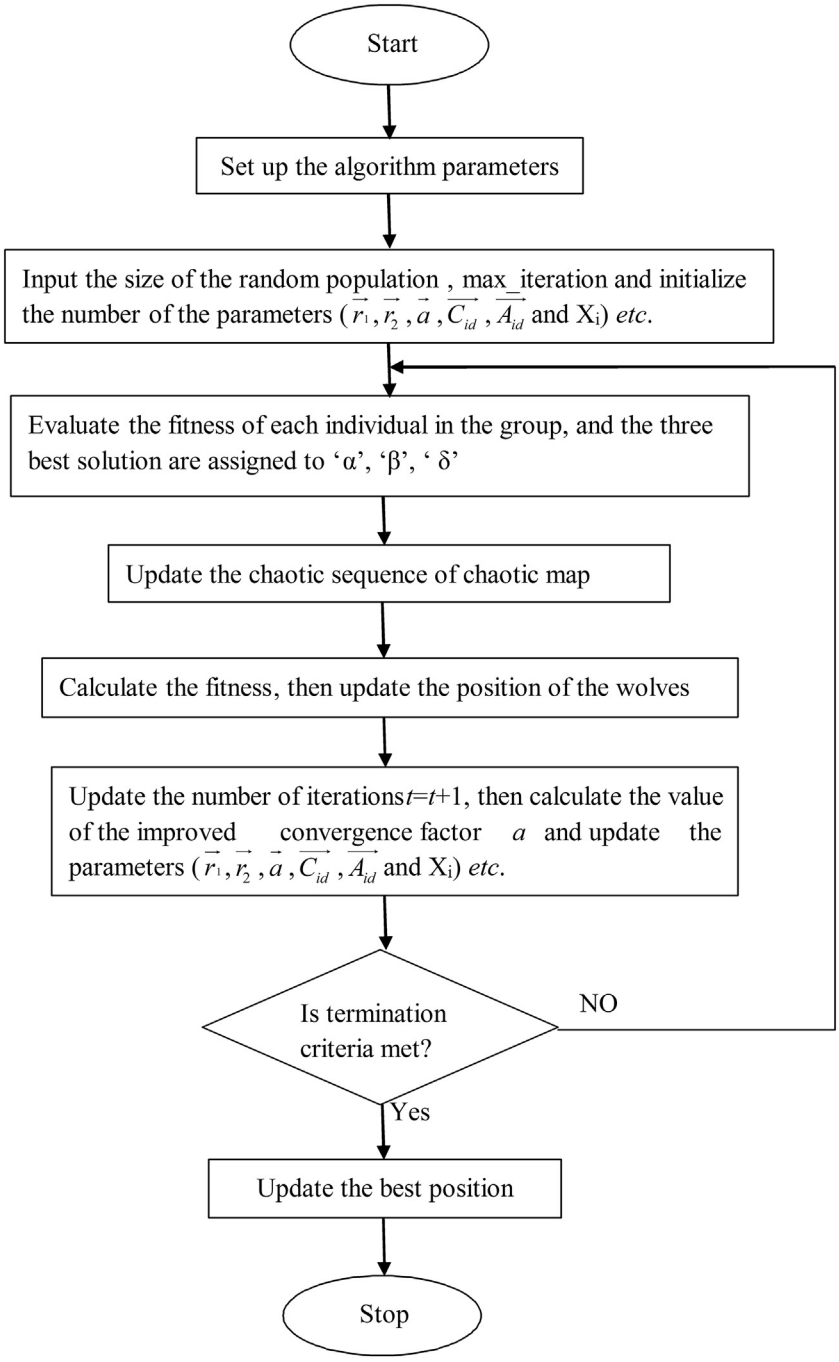

Fig. 1. The flowchart of ACGWO.

2.4. UHPLC-IT-TOF MS determination

The phytochemical analysis was performed using a Shimadzu LCMS-IT-TOF instrument that included a binary pump (LC-30AD), auto-sampler (SIL-30AC), DGU-30A3 de-gasser, photodiode array detector (SPD-M20A), communication base module (CBM-20A), column oven (CTO-30AC), ESI ion source, and IT-TOF mass spectrometer (Kyoto, Japan). The analytical column was a Thermo HyPURITY C_{18} (5 μm, 150 × 2.1 mm). The mobile phase was consisted of (A) water and (B) acetonitrile using a gradient elution of 15–60% B in 0–40 min, 60% B in 40–60 min, 60–15% B in 60–80 min, 15% B in 80–95 min. All mobile phases were filtered through a 0.22 μm membrane and degassed ultrasonically before use. The flow rate was set at 0.8 mL min^{-1}. The IT-TOF MS apparatus (Shimadzu, Kyoto, Japan) was operated in the positive ion mode scanning from *m/z* 100 to 1000, and the sampling frequency was set as 1.5625 Hz. The MS^2 ionization energy was set as 100–320%.

2.5. Cell viability test (CCK-8 detection)

THP-1 macrophages were cultured to exponential phase (1×10^5 cells/mL) and divided into groups in which 100 μL H_2O_2, SCC extract from CSS, SCC extract from *Ligusticum chuanxiong hort* and essential oil from *Rhizoma cyperi*, with different concentrations (5, 10, 20, 40, 80, 160 μg·mL^{-1}) were added and incubated for 3 h, respectively. After the addition of 10 μL CCK-8, the culture solution was incubated for 1 h. After washing three times, 100 μL DMSO was added to dissolve the precipitate. Then the solution was measured at 450 nm, and the

survival rate was calculated as follows:

$$\text{Cell viability}(\%) = \frac{\text{OD (Experimental group)}}{\text{OD (Control group)}} \times 100\% \quad (2)$$

2.6. Anti-inflammatory test

THP-1 cells were cultured in RPMI1640 medium containing 2% Fetal Bovine Serum (FBS), penicillin-streptomycin at 37 °C in a humidified 5% CO_2 atmosphere. The cellular differentiation was proceeded on RPMI1640 medium containing 100 ng/mL phorbol ester, 0.3% bovine serum albumin for 24 h. Drugs used for the study were dissolved in 100% DMSO, but the actual concentration of DMSO in treated plate is equal to or below 0.1%. 1 μg/mL Lipopolysaccharide (LPS) -evoked inflammation was taken place in macrophages, in which IL-6 and TNF-α were determined.

2.7. Antioxidant test

Hep G2 cells were cultured in Dulbecco's Modified Eagle's Medium (DMEM), penicillin-streptomycin at 37 °C in a humidified 5% CO_2 atmosphere for 24 h. Drugs used for the study were dissolved in 100% DMSO, but the actual concentration of DMSO in treated plate is equal to or below 0.1%. 0.03% H_2O_2 was added in the experimental and model groups, and DCFH-DA fluorescent probe was used to detect intracellular ROS.

3. Results and discussion

3.1. SCC extraction and structure analysis

By calculating and comparing the EY of CSS oil, the results showed that the maximum EY of 3.288% (w/w) was obtained by SCC extraction, while the extraction of hydro-distillation was 1.091% and the Soxhlet extraction was 2.475%. The surface structure of herbal particles was analyzed by Scanning Electron Microscopy (SEM). It can be seen from the Fig. S I2 (a) that the surface of the non-extracted herbs exhibits unevenness and extreme fullness, where the oil and non-extracted solid phases are in close contact with each other (Fig. S I2, Supplemental information I). In contrast, the extracted herbs clearly show the rupture and withering of the material layer, as shown in Fig. S I2 (b). The fact indicated that the herb layer is more easily broken to obtain the components under high pressure.

3.2. Modeling and prediction using RSM

Many parameters are directly or indirectly affect EY, so the analysis of the interaction between the variables is an important step in the SFE study. The preliminary study was based on three independent variables: pressure, temperature and particle size. It can be deduced from the AOV statistical analysis that the pressure, temperature, and particle size significantly affected the EY ($p < 0.05$). Among them, the pressure poses positive linear effect, while the temperature and particle are negative. The quadratic polynomial fitting equation is established by calculating the regression coefficients of the intercept, linear, quadratic and cross terms of the model by least squares method. The results indicated that the equation is in full compliance with the fitting requirements. In addition, a scatter plot in Fig. S I3 (Supplemental information I), the experimental EY were compared with the predicted EY, which suggested that the model is consistent with the actual data. The quadratic polynomial model is as follows:

$$\begin{aligned}\text{Yield} = {} & 2.88 - 0.18X_1 + 0.44X_2 - 0.14X_3 + 0.11X_1X_2 - 0.11X_1X_3 \\ & - 0.58X_2X_3 + 0.12X_1^2 - 0.37X_2^2 - 0.83X_3^2 \end{aligned} \quad (3)$$

3.3. Effect of individual parameter on EY

In Fig. S I4 (Supplemental information I), effects of each parameter on EY could be clearly observed. During a given range, EY decreases with increasing temperature due to changes in the density of supercritical CO_2 fluid. On the contrary, the pressure has two opposite effects on the EY. This effect can be explained by the fact that the solubility of oils in SCC increases at higher pressure, but the mass transfer coefficients decrease with a rise in pressure. Similarly, the particle size also exerted two opposite influence on the EY. From the further observation of Fig. S I4, the effect of pressure and particle size on EY is more sensitive than that of temperature on EY.

3.4. Effect of 2-parameter interactions on EY

Fig. 2(a)–(c) indicates that all the input parameters in this study are involved in the interaction. By using the linear, quadratic and interactive terms in the second order polynomial model, the three-dimensional (3D) response surface and the two-dimensional contour map are drawn. The 3D response surface diagram helps to analyze the direction of the desired response, and vividly displays the fitted surface as the maximum, minimum or saddle point, but does not directly determine the parameter level. In the contour map, curves of equal response values were plotted on a plane where the coordinates represent the levels of the independent variables, and each value can be achieved more easily.

Fig. 2(a) reflects the impact of temperature (X1) and pressure (X2) on the EY at fixed particle size (X3). When the pressure is < 310 bar, the EY increases as the pressure increases. When the pressure is > 310 bar, the EY decreased slowly with the increase of the pressure. This phenomenon indicates that the pressure has a substantial positive effect on the EY with the change in the solubility of supercritical CO_2. On the one hand, the increased solubility of the essential oil/SC-CO_2 fluid was caused by the increase of pressure, because the interaction between the oil and CO_2 molecules increases. On the other hand, the diffusion coefficient also decreased as the pressure increased, leading to the reduce of EY.

Fig. 2(a) and (c) indicated that the increased temperature had a negative effect on the EY of essential oil. On the one hand, an increase in temperature can lead to a decrease in CO_2 density, when other parameters were fixed. On the other hand, the increased temperature may result in higher vapor pressure of essential oil, as well as the more solubility in SC-CO_2 fluid. In our test, the reduction of density exerts greater influence than the increase of vapor pressure.

Fig. 2(b) reflects the impact of temperature (X1) and particle size (X3) on the EY at a fixed pressure (X2). It is obvious that the particle size may have two different impacts on EY. On the one hand, the decreased particle size leads to an expanding surface area, and the expanding contact surface between the supercritical fluid and the herbs increases the EY. On the other hand, being too small, a particle size may cause insufficient contact between the particles and the SC-CO_2 fluid, leading to a decrease in EY. Eventually, internal Mass Transfer Resistance (MTR) and external MTR can reasonably explain the influence of particle size on EY.

$$\text{MSE} = \frac{1}{n}\sum_{i=1}^{n}(Y_{i,\text{mod}} - Y_{i,\text{exp}})^2 \quad (4)$$

$$\text{RMSE} = \sqrt{\frac{1}{n}\sum_{i=1}^{n}(Y_{i,\text{mod}} - Y_{i,\text{exp}})^2} \quad (5)$$

$$\text{AAD}(\%) = \frac{1}{n}\sum_{i=1}^{n}\left(\left|\frac{(Y_{i,\text{mod}} - Y_{i,\text{exp}})}{Y_{i,\text{exp}}}\right|\right) \times 100 \quad (6)$$

Three kinds of statistical parameters, mean square error (MSE) (4), root mean square error (RMSE) (5) and absolute average deviation

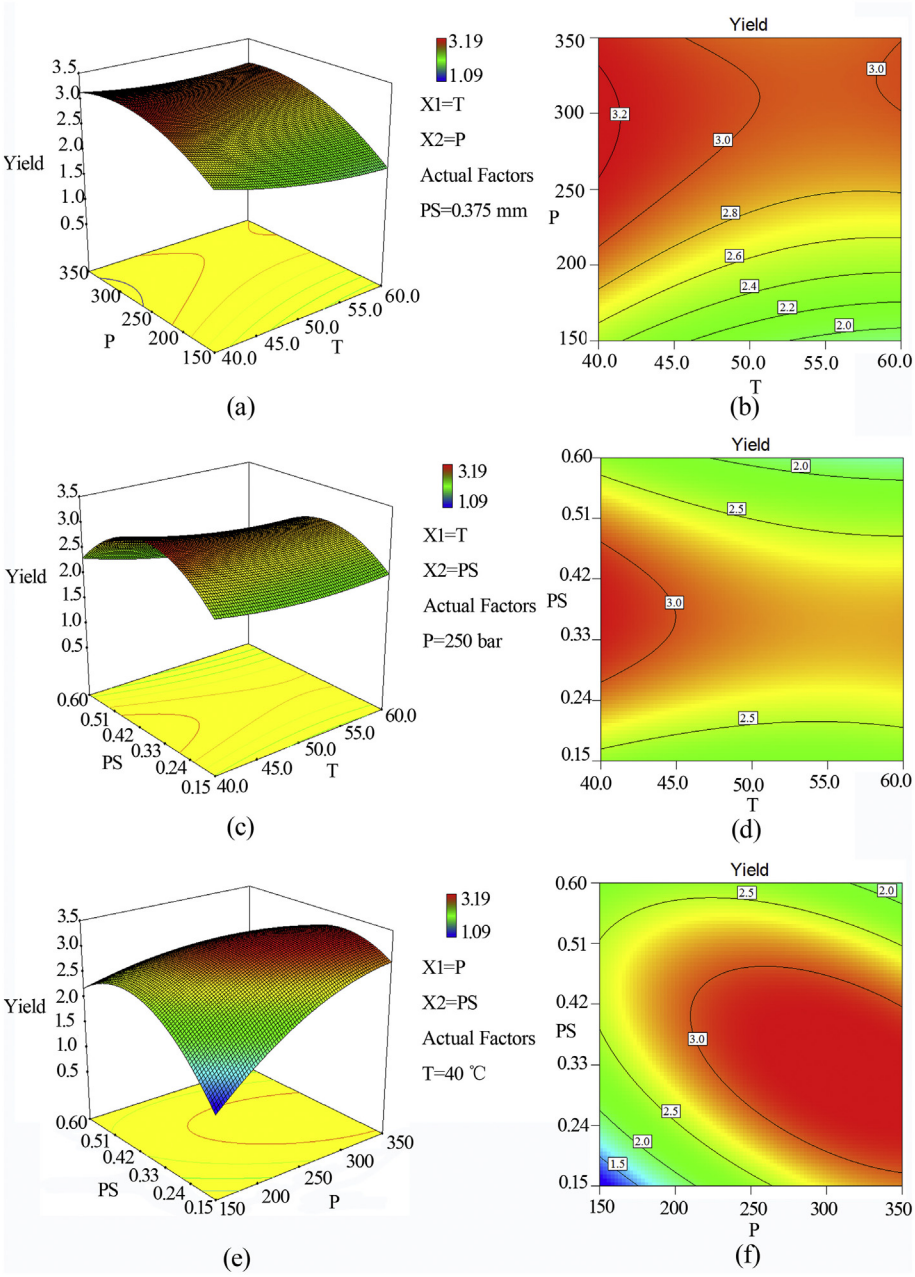

Fig. 2. (a) is the 3D response surface and contour plots for the effect of temperature (X_1) and pressure (X_2). (b) is the 3D response surface and contour plots for the effect of temperature (X_1) and particle size (X_3). (c) is the 3D response surface and contour plots for the effect of pressure (X_2) and particle size (X_3).

(AAD) (6) were calculated to estimate the accuracy of the model. Where $Y_{i,mod}$ and $Y_{i,exp}$ are EY values obtained by the model and the experiment, respectively; n is the number of experimental data. The data analysis draws the conclusion that the RSM model can accurately forecast the experimental data. The accuracy of the model is evaluated by calculating the corresponding error criteria, such as MSE, RMSE and AAD, that were calculated as 0.00060728, 0.02464, 0.70508%, respectively.

3.5. Optimization by ACGWO method

In this study, three factors, such as extraction temperature (40–60 °C), extraction pressure (150–350 bar) and particle size (0.15–0.60 mm), were selected after a comprehensive consideration. After the SCC extraction, the quadratic polynomial model of EY is obtained by RSM analysis. The model was further optimized by ACGWO algorithm, leading to the optimal EY and parameters. The results showed that the maximum EY is 3.2881% (w/w), and the corresponding parameters are 40 °C, 313.422 bar and 0.320 mm.

The results of GWO, PSO, the nonlinear convergence factor a introduced in the basic GWO algorithm (AGWO), the Chaotic Grey Wolf Optimization (CGWO) and ACGWO were compared. It is concluded that the PSO result is local optimum rather than global optimal solution, yet the results obtained by GWO, AGWO, CGWO and ACGWO are consistent.

The advantages and disadvantages of the optimization algorithms are not only reflected in the accuracy, but also in the stability. The stability and deviation calculation of the GWO, PSO, AGWO, CGWO and ACGWO algorithms were 3.2812 ± 0.01190, 3.2217 ± 0.01159, 3.2855 ± 0.00504, 3.2856 ± 0.00481 and 3.2857 ± 0.00447. The

results showed that the basic GWO algorithm is inferior to the PSO algorithm in terms of stability. To tackle this problem, one nonlinear convergence factor *a* was introduced. On the one hand, the algorithm is more suitable for actual circumstances. On the other hand, the balance between global search ability and local search ability can be achieved in the process of fast convergence. The results also indicated that the application of nonlinear convergence factor made the optimization of EY model more rapid and stable.

The chaos theory is introduced to improve the initial population of GWO to ensure the initial population diversity in the search process. The results showed that the introduction of chaos algorithm in GWO can enhance the accuracy of the algorithm and prevent it from falling into the local optimal solution. At the same time, it is found that convergence speed is enhanced at the cost of the stability of the algorithm, after the comparison (standard deviation) between CGWO and AGWO algorithm. Therefore, nonlinear convergence factor and chaos theory should be integrated to ensure not only a faster convergence rate, but also a better balance between the local search and global search, avoiding falling into local best points.

The convergence of the GWO, PSO, AGWO, CGWO and ACGWO algorithm were compared in Fig. S I5 (Supplemental information I). It can be seen from the figure that with the increase of the number of iterations, the adaptability of the global optimal solution increases. GWO stabilized at 3.2881 after 15 generations, while the PSO algorithm stabilized at 3.2284 after 20 generations, consistent with the literature information. By introducing the chaos theory, the CGWO algorithm is stable at the minimum value of 3.2881 after 10 generations, which accelerates the convergence rate of the algorithm. Fig. S I5 clearly illustrates that ACGWO can both speed up the convergence rate and guarantee the stability of the algorithm. Therefore, ACGWO is a more efficient and feasible algorithm.

3.6. GC-CI-MS and UHPLC-IT-TOF MS determination

The yellow oil-like extracts from the separator I and separator II, have been subjected to a further GC-EI-MS test [3]. In this study, GC-CI-MS was used to further confirm the molecular formula of some components in the SCC extract, thereby further narrowing the search window. Take peak 11 (*m/z* 133, 105, 77) as an example, a lot of candidates were searched in NIST 14 database which annotated with $C_{15}H_{20}O$, $C_{12}H_{14}O_2$, $C_{12}H_{14}O_3$ and $C_{12}H_{16}O$. Through the protonation ion determination by GC-CI-MS, 3-Butylphthalide ($C_{12}H_{14}O_2$) was searched out. Finally, the main chemical composition obtained by SC-CO_2 extraction is presented in Fig. 3.

For the non-volatile components, LC–MS can effectively detect them in positive/negative mode. Here, UHPLC-IT-TOF MS was used to analyze the phytochemicals in the SCC extract. The ion chromatograms showed that the response of phytochemicals in the positive mode far beyond those in the negative mode. After accurate mass determination, the candidates were selected from an in-house database. Then their MS^2

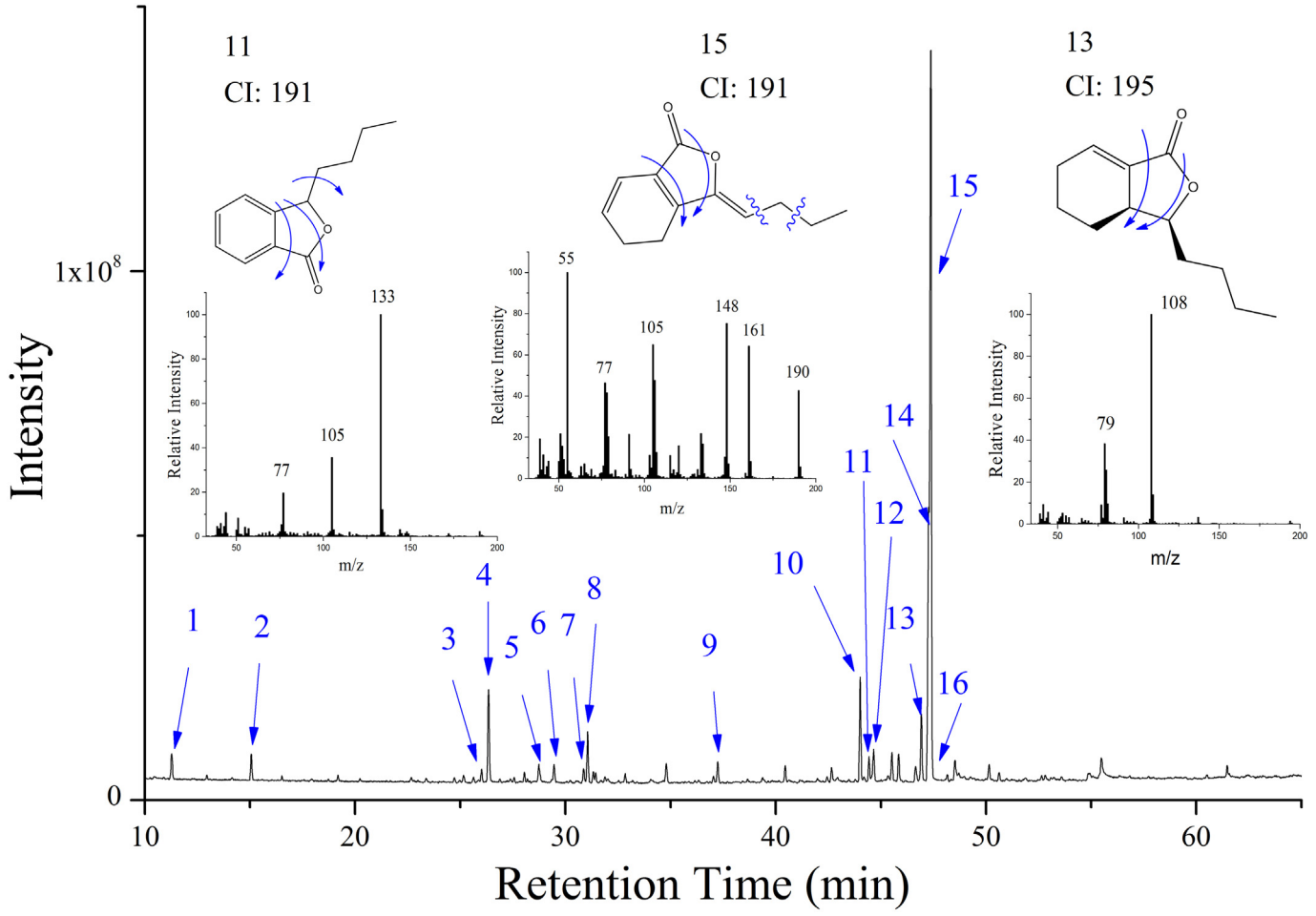

Fig. 3. GC-EI/CI-MS analysis for SCC extraction from CSS.
1) D-Limonene; 2) Linalool; 3) β-Elemene; 4) α-Gurjunene; 5) 2-Methoxy-4-vinylphenol; 6) Rotundene; 7) Germacrene D; 8) β-Selinene; 9) Caryophyllene oxide; 10) Cyperenone; 11) Butylphthalide; 12) Butylidenephthalide; 13) Neocnidilide; 14) Senkyunolide; 15) (*Z*)-Ligustilide.

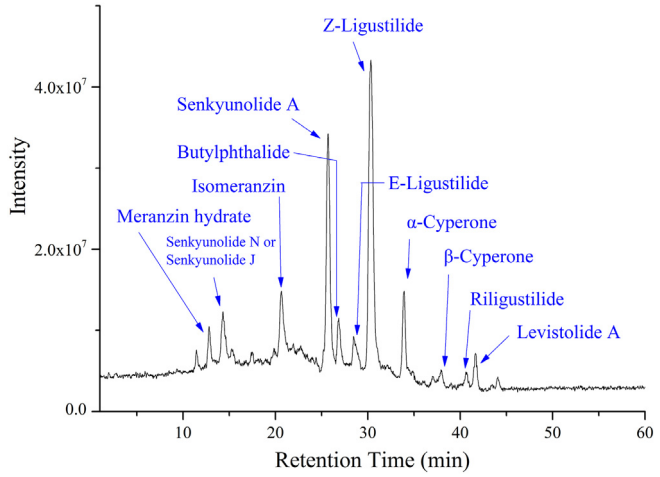

Fig. 4. LC- IT-ToF-MS analysis result for SCC extract from CSS.

fragmental patterns were recognized, leading to the identification of most compounds. As seen in Fig. 4, *Z*-Ligustilide and other phthalides are mainly responsible for the SCC extract; the next is α-Cyperone in *Cyperus rotundus*; again is Meranzin hydrate, Isomeranzin in *Citrus reticulata Blanco*. The specific data can be seen in Table S1 (Supplemental information III).

3.7. Anti-inflammatory test

As seen in Fig. 5(a), the cell viability measured by CKK-8 showed that the sample or LPS can't affect the cell viability within a certain concentration range. That is to say, the SCC extract from CSS, the SCC extract from *Ligusticum chuanxiong hort* and the essential oil from *Rhizoma cyperi*, have no cytotoxicity on cells in the experimental procedure. As seen from Fig. 5(b) and (c), THP-1 macrophages were used to detect the pharmacological effects of herbal extracts on the production of proinflammatory cytokines. After the inflammation-stimulation by LPS (1 μg/mL) for 24 h, the expression of IL-6 and TNF-α increased with the incubation time. When incubating with the herb extracts and LPS for 24 h, the expression of IL-6 and TNF-α could be effectively reduced. As shown in Fig. 5(b) and (c), the expression of IL-6 and TNF- α showed a positive correlation with the dose (2 μg/mL, 10 μg/mL, 20 μg/mL and 40 μg/mL) of three samples. Among them, the SCC extract from CSS, the SCC extract from *Ligusticum chuanxiong hort* and the essential oil from *Rhizoma cyperi* had significant inhibitory effects on the inflammatory factor IL-6; and the higher the concentration of the sample, the stronger the inhibition effect. The SCC extract from *Ligusticum chuanxiong hort* has a certain inhibitory effect on cytokine TNF-α; and increases with the herbal accumulation. However, the SCC extract from CSS and the essential oil from *Rhizoma cyperi* have no obvious effect on cell inflammatory factor TNF-α. Therefore, the anti-inflammatory effect of the SCC extract from CSS is mainly exerted by inhibiting the production of IL-6.

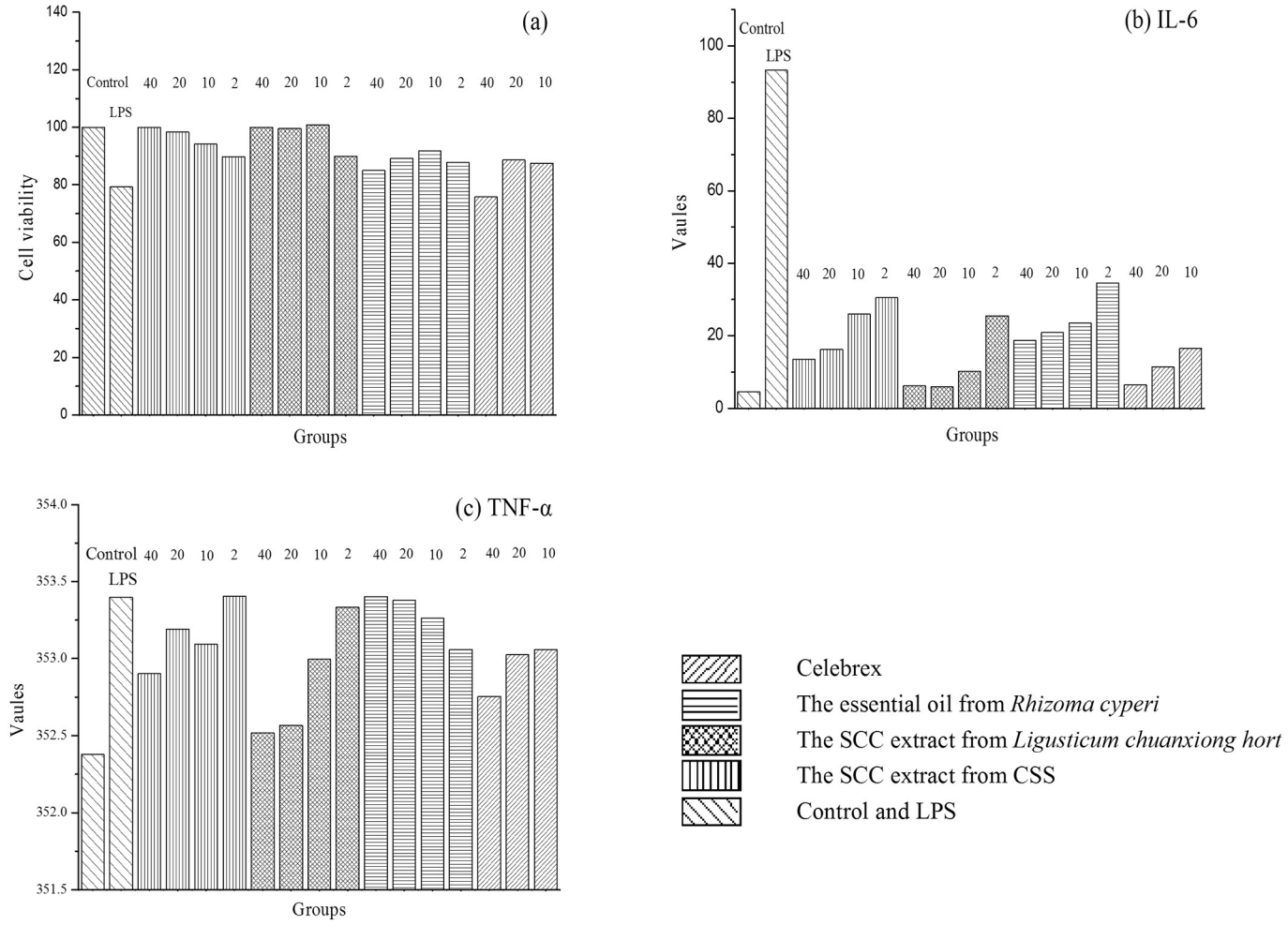

Fig. 5. The cell viability (a), the expression of IL-6 (b) and TNF-α (c) after the incubation with herbal extracts.

3.8. Antioxidant test

The effects of the SCC extract from CSS, the SCC extract from *Ligusticum chuanxiong hort* and the essential oil from *Rhizoma cyperi* on ROS content in a cell model with oxidative stress, can be seen in Fig. 6. The results showed that the ROS was obviously enhanced after an incubation with H_2O_2 for 1 h. It also indicated that H_2O_2 could accelerate the oxidative stress of the cells, that is, the oxidative stress model was established. After an incubation for 24 h, the herbal extracts could effectively reduce the content of ROS, and positively correlated with the dosage. In Fig. 6, the concentration of ROS is shown with the samples of 10 μg/mL, 20 μg/mL, 40 μg/mL, 80 μg/mL and 160 μg/mL. The results showed that the SCC extract from CSS, the SCC extract from *Ligusticum chuanxiong hort* and the essential oil from *Rhizoma cyperi* have significant inhibitory effects on the oxidative stress of the cells, by a positive correlation with dosage. By contrast, the antioxidant effect of the SCC extract from *Ligusticum chuanxiong hort* is better than that of the SCC extract from CSS and the essential oil from *Rhizoma cyperi*. At the concentration of 160 μg/mL, the SCC extract from CSS, the SCC extract from *Ligusticum chuanxiong hort* exert the most significant antioxidant activity; yet the best concentration of the essential oil from *Rhizoma cyperi* is 20 μg/mL.

After 24 h incubation with the SCC extract from CSS, 0.03% H_2O_2 was added in the culture mediums, then ROS variations within 1 h can be observed in Fig. 6c. The curve slope can indicate the strength of antioxidant activity, the lower the slope and the stronger antioxidant effect. As from Fig. 6c, the ROS slope of the SCC extract from CSS with different concentrations was significantly lower than that of the model group, and the higher the drug concentration, the stronger the antioxidant effect.

4. Conclusion

In this work, seven herbs were simultaneously extracted by SCC in a rapid and environmental-friendly manner. To solve the real-world problems, an ACGWO algorithm was used to optimize the EY model established by RSM. Subsequently, the morphology examination indicated that the herb layer is more easily broken to obtain the components under high pressure. Through the LC-IT-Tof-MS determination, the components of this product were come from *Ligusticum chuanxiong hort*, *Rhizoma cyperi* and *Citrus reticulata*, especially phthalides. In two cell models, the SCC extract was proved to possess the pharmacological activities of anti-inflammatory and antioxidant. It is worth mentioning that these significant activities are closely related to those of *Ligusticum chuanxiong hort* and *Rhizoma cyperi*.

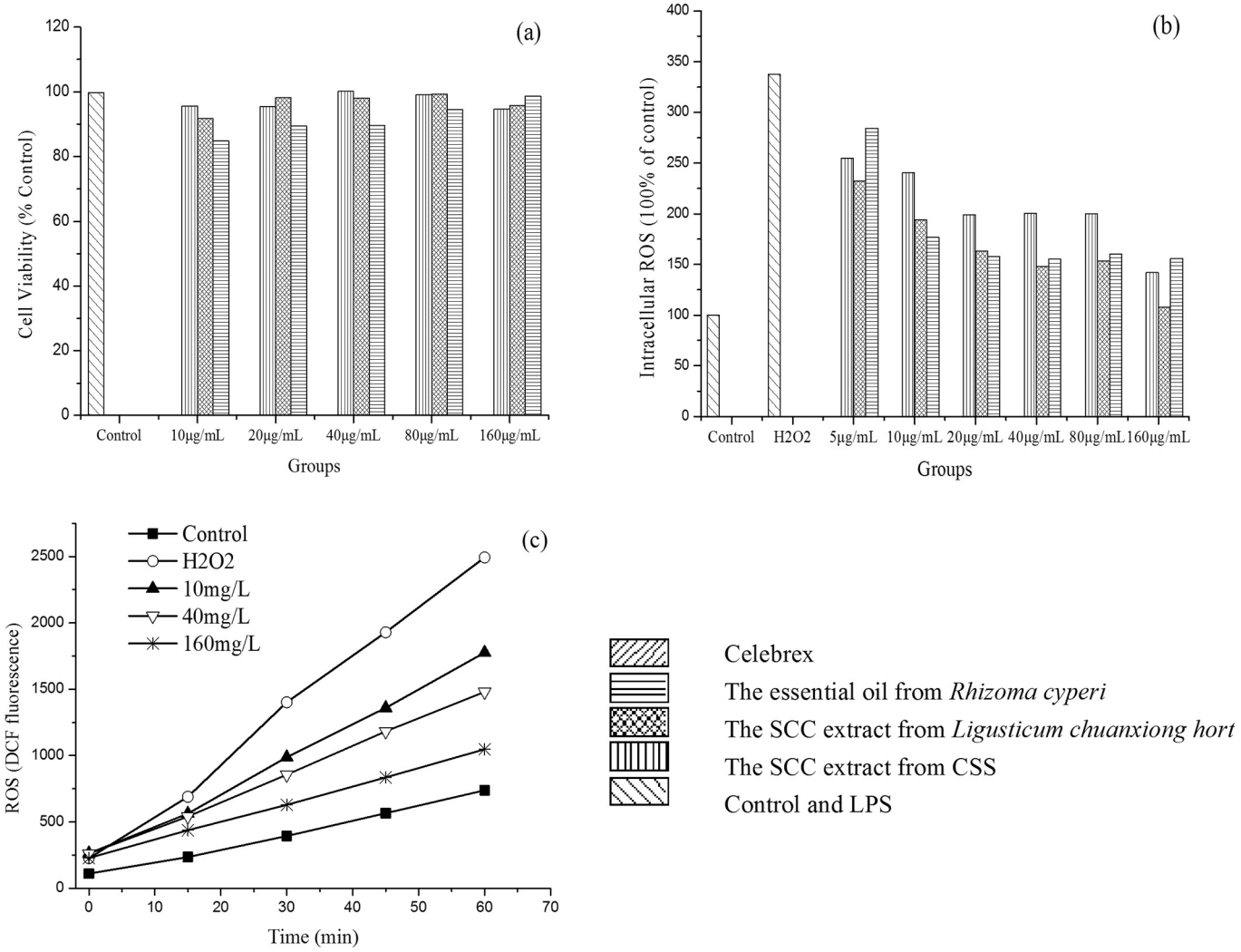

Fig. 6. The cell viability (a), the effects of herbal extracts on ROS content in a cell model with oxidative stress (b), the ROS slope of the SCC extract from CSS with different concentrations (c).

Disclosure statement

No potential conflict of interest was reported by the authors.

Acknowledgement

This work is financially supported by Hunan 2011 Collaborative Innovation Center of Chemical Engineering & Technology with Environmental Benignity and Effective Resource Utilization, Hunan Province Natural Science Fund (no. 2016JJ4085), the college students' science and technology innovation project (2016sj010). The studies meet with the approval of the university's review board.

We appreciate Dr. Yi Cao for his scientific assistance in cell studies.

Appendix A. Supplementary data

Supplementary data to this article can be found online at https://doi.org/10.1016/j.microc.2018.07.016.

References

[1] X. Huang, Y. Guo, W.H. Huang, W. Zhang, Z.R. Tan, J.B. Peng, Y.C. Wang, D.L. Hu, D.S. Ouyang, J. Xiao, Y. Wang, M. Luo, Y. Chen, Searching the cytochrome p450 enzymes for the metabolism of meranzin hydrate: a prospective antidepressant originating from Chaihu-Shugan-San, PLoS One 9 (2014) e113819.

[2] S. Chen, T. Asakawa, S. Ding, L. Liao, L. Zhang, J. Shen, J. Yu, K. Sugiyama, H. Namba, C. Li, Chaihu-Shugan-San administration ameliorates perimenopausal anxiety and depression in rats, PLoS One 8 (2013) e72428.

[3] M. He, Z.Y. Yang, T.b. Yang, Y. Ye, J. Nie, Y. Hu, P. Yan, Chemometrics-enhanced one-dimensional/comprehensive two-dimensional gas chromatographic analysis for bioactive terpenoids and phthalides in Chaihu Shugan San essential oils, J. Chromatogr. B 1052 (2017) 158–168.

[4] J. Mejri, M. Abderrabba, M. Mejri, Chemical composition of the essential oil of *Ruta chalepensis* L: influence of drying, hydro-distillation duration and plant parts, Ind. Crop. Prod. 32 (2010) 671–673.

[5] M.E. Lucchesi, F. Chemat, J. Smadja, Solvent-free microwave extraction of essential oil from aromatic herbs: comparison with conventional hydro-distillation, J. Chromatogr. A 1043 (2004) 323–327.

[6] R.S. Ayala, M.D.L. de Castro, Continuous subcritical water extraction as a useful tool for isolation of edible essential oils, Food Chem. 75 (2001) 109–113.

[7] G.C. Moreira, F.S. Dias, Mixture design and Doehlert matrix for optimization of the ultrasonic assisted extraction of caffeic acid, rutin, catechin and trans-cinnamic acid in *Physalis angulata* L. and determination by HPLC DAD, Microchem. J. 141 (2018) 247–252.

[8] M.M.R. de Melo, P.F. Martins, A.J.D. Silvestre, Pedro Sarmento, C.M. Silva, Measurement and modeling of supercritical fluid extraction curves of *Eichhornia crassipes* for enhanced stigmasterol production: mechanistic insights of the process, Sep. Purif. Technol. 163 (2016) 189–198.

[9] R.N. Núñez, A.V. Veglia, N.L. Pacioni, Improving reproducibility between batches of silver nanoparticles using an experimental design approach, Microchem. J. 141 (2018) 110–117.

[10] T. Şahan, F. Erol, Ş. Yılmaz, Mercury(II) adsorption by a novel adsorbent mercapto-modified bentonite using ICP-OES and use of response surface methodology for optimization, Microchem. J. 138 (2018) 360–368.

[11] A. Cabeza, F. Sobrón, J. García-Serna, M.J. Cocero, Simulation of the supercritical CO2 extraction from natural matrices in packed bed columns: user-friendly simulator tool using excel, J. Supercrit. Fluids 116 (2016) 198–208.

[12] E.L.C. Cheah, P.W.S. Heng, L.W. Chan, Optimization of supercritical fluid extraction and pressurized liquid extraction of active principles from Magnolia officinalis using the Taguchi design, Sep. Purif. Technol. 71 (2010) 293–301.

[13] A. Guardo, M. Coussirat, F. Recasens, M.A. Larrayoz, X. Escaler, CFD studies on particle-to-fluid mass and heat transfer in packed beds: free convection effects in supercritical fluids, Chem. Eng. Sci. 62 (2007) 5503–5511.

[14] S. Mirjalili, S.M. Mirjalili, A. Lewis, Grey Wolf Optimizer, Adv. Eng. Softw. 69 (2014) 46–61.

[15] M.S. Li, X.Y. Huang, H.S. Liu, B.X. Liu, Y. Wu, L.J. Wang, Solubility prediction of supercritical carbon dioxide in 10 polymers using radial basis function artificial neural network based on chaotic self-adaptive particle swarm optimization and K-harmonic means, RSC Adv. 56 (2015) 45520–45527.

[16] T. Hatami, M.A.A. Meireles, G. Zahedi, Mathematical modeling and genetic algorithm optimization of clove oil extraction with supercritical carbon dioxide, J. Supercrit. Fluids 51 (2010) 331–338.

[17] J.A. Lazzús, Hybrid particle swarm-ant colony algorithm to describe the phase equilibrium of systems containing supercritical fluids with ionic liquids, Commun. Comput. Phys. 14 (2013) 107–125.

[18] G. Sodeifian, N. Saadati Ardestani, S.A. Sajadian, S. Ghorbandoost, Application of supercritical carbon dioxide to extract essential oil from Cleome coluteoides Boiss: experimental, response surface and grey wolf optimization methodology, J. Supercrit. Fluids 114 (2016) 55–63.

[19] Y. Shen, S. Lin, C. Han, Z. Zhu, X. Hou, Z. Long, K. Xu, Rapid identification and quantification of five major mogrosides in *Siraitia grosvenorii* (Luo-Han-Guo) by high performance liquid chromatography–triple quadrupole linear ion trap tandem mass spectrometry combined with microwave-assisted extraction, Microchem. J. 116 (2014) 142–150.

[20] M. He, H. Wu, J. Nie, P. Yan, T.B. Yang, Z.Y. Yang, R. Pei, Accurate recognition and feature qualify for flavonoid extracts from Liang-wai Gan Cao by liquid chromatography-high resolution -mass spectrometry and computational MS/MS fragmentation, J. Pharmaceut. Biomed. 146 (2017) 37–47.

[21] L. Kuai, J.T. Zhang, Y. Deng, S. Xu, X.Z. Xu, M.F. Wu, D.J. Guo, Y. Chen, R.J. Wu, X.Q. Zhao, H. Nian, B. Li, F.L. Li, Sheng-ji Hua-yu formula promotes diabetic wound healing of re-epithelization via Activin/Follistatin regulation, BMC Complement. Altern. Med. 18 (2018) 32.

[22] H. Sui, P. Duan, P. Guo, L. Hao, X. Liu, J. Zhang, H. Zhu, M. Zhao, H. Wang, Q. Li, S. Wang, Zhi Zhen Fang formula reverses Hedgehog pathway mediated multidrug resistance in colorectal cancer, Oncol. Rep. 38 (2017) 2087–2095.

[23] Q. Zhou, Y. Wang, J. Zhang, Y. Shao, S. Li, Y. Wang, H. Cai, Y. Feng, W. Le, Fingerprint analysis of Huolingshengji formula and its neuroprotective effects in SOD1G93A mouse model of amyotrophic lateral sclerosis, Sci. Rep. 8 (2018) 1668.

[24] Z.N. Wu, Y.B. Zhang, N.H. Chen, M.J. Li, M.M. Li, W. Tang, L. Zhuang, Y.L. Li, G.C. Wang, Sesquiterpene lactones from *Elephantopus mollis* and their anti-inflammatory activities, Phytochemistry 137 (2017) 81–86.

[25] W. Ding, J. Gu, L. Cao, N. Li, G. Ding, Z. Wang, L. Chen, X. Xu, W. Xiao, Traditional Chinese herbs as chemical resource library for drug discovery of anti-infective and anti-inflammatory, J. Ethnopharmacol. 155 (2014) 589–598.

[26] S. Rashid, M. Ahmad, M. Zafar, Asad Anwar, S. Sultana, S. Tabassum, S.N. Ahmed, Ethnopharmacological evaluation and antioxidant activity of some important herbs used in traditional medicines, J. Tradit. Chin. Med. 36 (2016) 689–694.

[27] H. Bendif, M.D. Miara, Zahar Kalboussi, D. Grauzdytė, D. Povilaitis, P.R. Venskutonis, Filippo Maggi, Supercritical CO2 extraction of *Rosmarinus eriocalyx* growing in Algeria: chemical composition and antioxidant activity of extracts and their solid plant materials, Ind. Crop. Prod. 111 (2018) 768–774.